ICONHIC2019
2nd International Conference on Natural Hazards & Infrastructure
23-26 June, 2019, Chania, Greece

Seabed foundation of jacket wind-platforms

M. Antoniou
ETH Zurich, Switzerland

F. Gelagoti[1], R. Kourkoulis
National Technical University of Athens, Greece

S. A. Karamanos
University of Thessaly, Greece
University of Edinburgh, UK

ABSTRACT

The paper introduces a cost-effective and 'easy-to-install' foundation concept to be used for the seabed support of jacket wind-platforms. The concept, commonly termed as 'suction caisson' is a skirt foundation (i.e. a stiff cylindrical shell with an open bottom and a top slab) that is particularly advertised for the ease of installation and the minimization of installation noise compared to piles. Aiming to raise the barriers towards their implementation, the paper initially illustrates the key parameters controlling the response of suction caissons under dynamic loading, by means of a dimensional analysis and a subsequent parametric study. The caissons are shown to behave excellently when subjected to pure dynamic loading, displaying only minimal permanent displacements. Alarming issues for their performance arise when a non-zero steady force is superimposed to the subsequent dynamic loading. In the case of concurrent static and seismic loading, analyses results reveal that the rate and amplitude of the irrecoverable caisson deformation is controlled by the amplitude of the initially imposed static action and the intensity of the earthquake motion.
Subsequently, an 8MW jacket-supported offshore wind-turbine (OWT) installed at a water depth site of 60m in the seismically active region of North-Western Adriatic is used as benchmark example to examine suction caisson behavior within the soil-structure system. The dynamic response of the benchmark OWT is numerically explored by exciting the system with a regional seismic record from the L' Aquila earthquake. As expected, the jacket is shown to behave excellently when subjected to pure earthquake loading, displaying minimal permanent foundation rotation. When earthquake loading is combined with a co-seismic wind action, jacket legs settle unevenly while the OWT tower builds-up rotations at an increasing rate.

Keywords: suction caissons, jacket structure, FE modelling, dimensional analysis, earthquake

INTRODUCTION

Foundations for offshore wind turbines (OWTs) are not merely a boundary condition but rather a crucial contributor to the endurance and serviceability of this promising infrastructure. As such, and given the fact that wind farms are moving into deeper waters, they have been the subject of substantial research during the last decades. Among them, suction caisson is gradually becoming popular in the offshore wind industry

[1] Corresponding author email: fanigelagoti@gmail.com

either as monopod or forming the base of multi-pod supporting structures (i.e. fixed jackets, tripods, tension leg platform systems).

Extensive research on the response of suction caissons has been conducted so far by means of field experiments (*Andersen et al, 1993; Dyvic et al, 1993*), centrifuge tests (*Clukey et al, 1993; 1995; Mana et al, 2012; 2013*), 1-g laboratory physical models (*Cauble 1996; Byrne 2003*), limit equilibrium methods (*Deng et al, 2002; Iskander et al, 2002; Randolph & Gourvenec, 2009*), and finite element analyses (*Bransby & Yun, 2009; Gourvenec & Barnett, 2011; Vulpe 2015; Keawsawasvong & Ukritchon, 2016; Mana & Gourvenec, 2013; Ukritchon & Keawsawasvong, 2016; Gelagoti et al, 2018; Ukritchon et al, 2018*). The majority of these studies have focused mainly on the undrained capacity under monotonic and cyclic loading taking into account the effect of foundation geometry, combined loading, installation process, different soil types and adhesion factor at the soil-caisson interface. To the authors' knowledge, only limited studies have tackled the subject of earthquake performance of such foundations; *Kourkoulis et al (2014)* evaluated the effect of soil-sidewall interfaces on the response of wind turbines founded on monopod suction caisson under monotonic lateral, cyclic and earthquake loading. More recently, *Wang et al (2017)* analyzed the seismic behavior of suction buckets through centrifuge modelling.

Recognizing that offshore wind farms construction is expanding worldwide, not excluding coastal regions of high seismicity (e.g., Pacific Coast, Gulf of Mexico, Adriatic Sea and Japan), the objective of this study is to elaborate further on the static and dynamic axial response of suction caissons through 3D finite element analyses. With respect to the state-of-the-art, our focus is primarily channeled to the comprehensive dimensional analysis and parametric study of axially-loaded suction caissons, assuming static, dynamic and concurrent static and seismic loading conditions. Finally, a benchmark example of an entire soil-jacket foundation-superstructure system is analyzed to provide further insight into the seismic performance of offshore wind turbines.

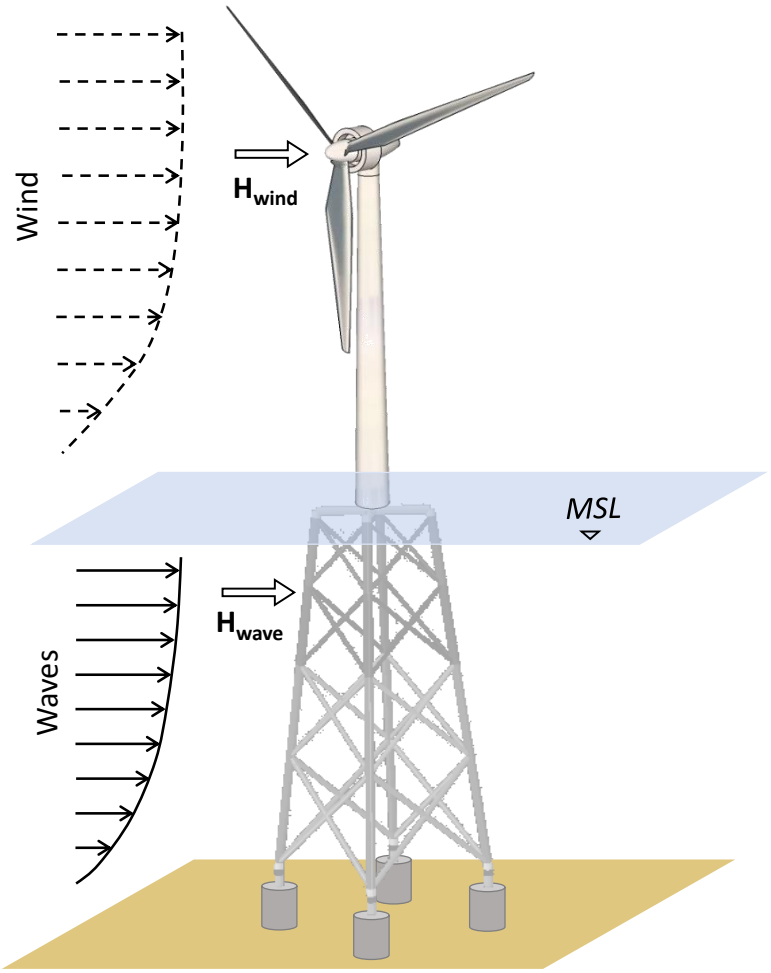

Figure 1. Problem Definition: Offshore wind turbine supported on a jacket structure tethered to the seabed by means of suction caissons.

DIMENSIONAL ANALYSIS OF SUCTION CAISSONS UNDER AXIAL LOADING

This section performs a formal dimensional analysis of suction caissons in clay, accounting for soil inelasticity and geometric nonlinearities. The derived formulations aim to highlight the key factors governing the behaviour of these foundations, under three load cases relevant to the ones experienced by the suction caissons supporting a jacket structure; namely: (a) Static axial loading (as imposed by dead loads and wind action), (b) dynamic axial loading (as imposed by waves action) and (c) concurrent static (due to wind action) and seismic loading.

The examined suction caisson configuration of length L and diameter D lies on a clayey soil deposit of depth z, constant undrained shear strength S_u, shear wave velocity V_s and density ρ. Regarding the development of negative excess pore pressures beneath the caisson lid, the assumption of "perfectly sealed" caissons is made herein: full suction conditions are developed beneath the caisson lid and a "reverse end bearing" mechanism takes place during uplift loading. The latter was deemed representative for the present study, as in cases of rapid loading like the ones examined herein (e.g. during an earthquake), the excess pore water pressures don't have time to dissipate and passive suction is maintained below the caisson lid. In the ensuing, a rigorous formulation of the dimensionless terms pertaining to the problem under consideration is attempted, starting from the simplest case of static loading.

The employed dimensional formulations are based on the Vaschy-Buckingham Π-theorem, according to which a dimensionally homogeneous equation involving k variables may be transformed to a function of k-n dimensionless Π-products, where n is the minimum number of reference dimensions necessary for the description of the physical variables. For the three cases examined, the total of independent physical variables involved in the problem are listed in Table 1: applied axial load N, caisson diameter D, length L, undrained shear strength S_u, soil Young's modulus E, soil density ρ, seismic acceleration α, and loading frequency f. Apparently, the foundation response shall not be a function of dynamic characteristics for the static case, i.e. acceleration and frequency.

The foundation settlement under static loading may be expressed as:

$$w_{st} = f\,(N, D, L, S_u, E) \tag{1}$$

Applying the Π-theorem on Equation (1), which contains k = 5 independent variables involving n = 2 reference dimensions (length, mass), one results in 3 dimensionless Π-products. Therefore, Equation (1) may be rearranged in dimensionless terms so that:

$$\frac{w_{st}}{D} = f\left(\frac{N}{S_u D^2}, \frac{L}{D}, \frac{E}{S_u}\right) \tag{2}$$

In order for Equation (1) to applicable for dynamic axial loading, k = 7 independent variables are considered, involving n = 3 reference dimensions (length, mass, time). This results in 4 dimensionless Π-products, such as:

$$w_{dyn} = f\,(N, D, L, S_u, E, \rho, f) \tag{3}$$

$$\frac{w_{dyn}}{D} = f\left(\frac{N}{S_u D^2}, \frac{L}{D}, \frac{E}{S_u}, \frac{f}{R}\right) \tag{4}$$

where: $R = \sqrt{E/\rho D L}$

Finally, for the seismic case, acceleration α is added to the set of independent variables. The latter corresponds to an effective acceleration value (different from the peak ground acceleration) estimated as the average acceleration amplitude of the strong motion part of the excitation. Moreover, for the ease of formulation, it is simplistically assumed that earthquake shaking may be described by one representative frequency – let it be the frequency corresponding to maximum spectral response of the seabed motion.
This yields:

$$w_E = f\,(N, D, L, S_u, E, \rho, a, f) \tag{5}$$

$$\frac{w_E}{D} = f\left(\frac{N}{S_u D^2}, \frac{L}{D}, \frac{E}{S_u}, \frac{f_E}{R}, \frac{S_u}{\rho L \alpha}\right) \quad (6)$$

All independent variables and postulated dimensionless products considered for the present dimensional analysis are summarized in **Table 1.**

Table 1. Suction caisson subjected to axial static, axial dynamic and a combination of axial static and seismic loading: Identification of dimensionless Π-products.

Independent Physical Variables			
N, D, L, S_u, E, ρ, α, f			
Dimensionless products			
Aspect Ratio:	$\frac{L}{D}$	Frequency ratio:	$\frac{f}{R}$ with $R = \sqrt{E/\rho D L}$
Soil rigidity ratio:	$\frac{E}{S_u}$	Soil strength mobilization index:	$\frac{S_u}{\rho L \alpha}$
Vertical capacity ratio:	$\frac{N}{S_u D^2}$		

Finite Element Modelling

The problem is solved numerically using the commercially available finite element software ABAQUS (Dassault Systèmes, 2013). The 3D finite element mesh is portrayed in Figure 2. Taking advantage of the problem's symmetry, half the geometry is modelled. A very fine discretization has been adopted for the first 6 layers of circumferential elements in the region of the soil-foundation interface and for a thin zone just below the foundation tip (which were found to control the FE predictions of the foundation response), while to increase computational efficiency, mesh coarseness increases as we move away from the foundation.

The model boundaries are positioned sufficiently remotely to ensure no boundary effects on the foundation response: two and a half diameters (2.5D) either side of the foundation for the lateral boundaries, and 1.5L beneath the tip of the foundation for the bottom boundary. The boundary conditions imposed at the model edges are: constraints of horizontal displacement towards any direction for the nodes at the lateral faces of the model (x and y directions), prevention of the out-of-plane movement of the face at the plane of symmetry and restriction of any displacement for the nodes at the bottom of the model.

Shell elements (S4) with elastic behavior are employed for the simulation of the suction caisson. The soil is modeled using 8-node hexahedral continuum elements (C3D8), obeying to a non-linear kinematic hardening constitutive model incorporating the Von Mises plasticity failure criterion and associated flow rule. The model is appropriate for the description of the non-linear hysteretic behavior of clayey materials and its capacity to simulate soil-structure interaction systems under cyclic and seismic loading has been extensively validated by Anastasopoulos et al. (2011). The soil rigidity ratio E/S_u, where E the zero-plastic strain modulus of soil, is assumed equal to 1800, corresponding to a moderately stiff soil profile. The contact conditions between the foundation, the surrounding and the encased soil are assumed fully bonded (i.e. rough in shear and no separation allowed), accounting for perfectly sealed conditions under undrained loading.

Dimensional Response Analysis of two example caissons

Two self-similar (i.e. described by the exact same dimensionless Π-terms) soil-caisson configurations, named hereafter Caisson A and Caisson B, are subjected to the three loading cases described above (Table 2). Their response is presented in Figs 3-5 using physical and dimensionless variables.

Static Loading

Caissons A and B are loaded to their pull-out capacity, obviously yielding two different curves with $N_{ult,A}$ = 33 MN and $N_{ult,B}$ = 18 MN respectively, for a vertical uplift w = 0.2 m (Fig. 3a). In dimensionless terms,

however, the two curves coincide, yielding the same maximum vertical capacity ratio N_{ult}/S_uD^2 = 9.5 (Fig. 3b). Results can, of course, be extended to the case of static push-down loading, since "perfectly sealed" caissons yield the same axial capacity in tension and compression.

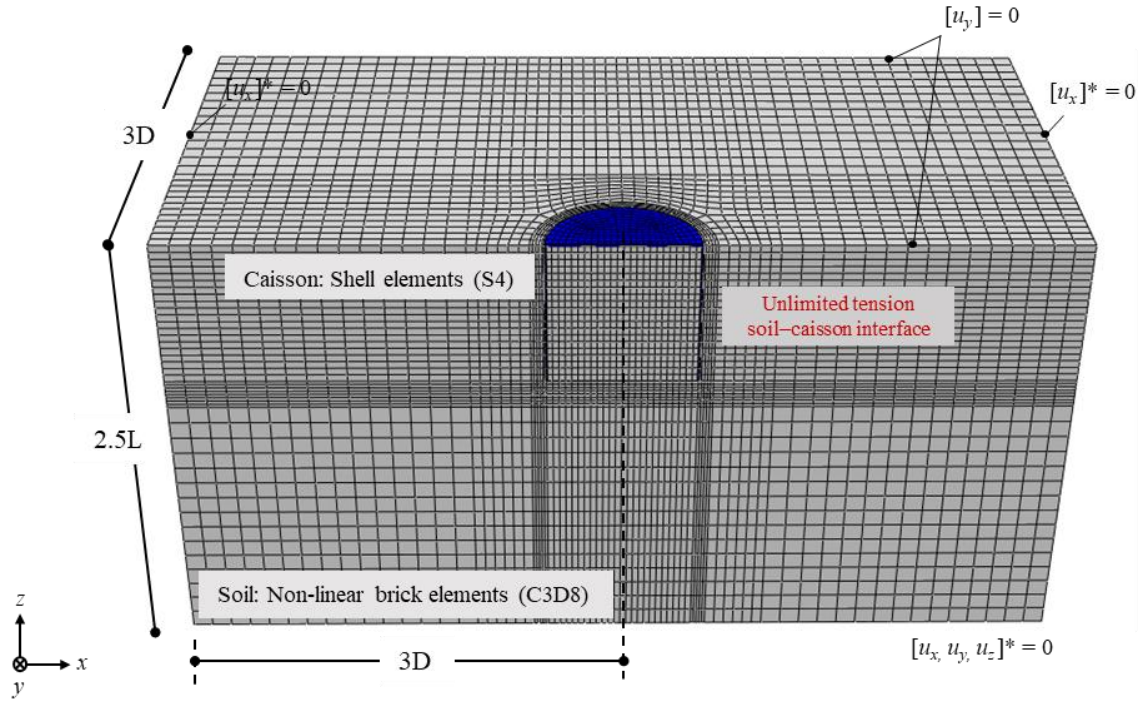

Figure 2. 3D FE model employed for the validation of the dimensional formulation

Table 2. Example Suction caissons: geometries and loading protocols.

Independent Variables			**Additional Independent Variables**		
Static Case:	**Caisson A**	**Caisson B**	*Dynamic Case:*	**Caisson A**	**Caisson B**
L (m)	6	5	f (Hz)	0.451	0.480
D (m)	6	5	R	42	45.1
S_u (kPa)	100	75	ρ (t/m^3)	1.835	1.65
E (kPa)	180000	135000	*Seismic Case:*	**Caisson A**	**Caisson B**
N (MN)	14.4	7.5	α_E (m/s^2)	0.659	0.659
			f_E (Hz)	0.71	0.76
Dimensionless products			**Additional Dimensionless products**		
Static Case:	L/D	1	*Dynamic Case:*	f/R	0.011
	E/S_u	1800	*Seismic Case:*	f_E/R	0.017
	N/S_uD^2	4		$S_u/\rho L\alpha_E$	13.8

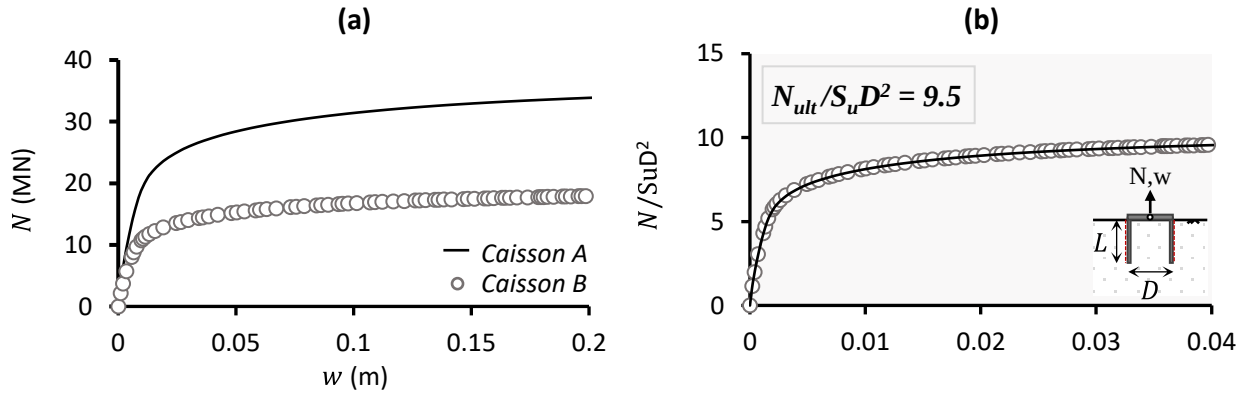

Figure 3. Validation of dimensional formulation. Pull-out load – displacement curves in (a) physical and (b) dimensionless terms.

Dynamic Loading

Caissons are loaded with 8 sinusoidal cycles at an absolute load amplitude that corresponds to $N/S_uD^2 = 4$ and frequencies $f_A = 0.451$ Hz and $f_B = 0.480$ Hz respectively resulting in the same frequency ratio $f/R = 0.011$ (Fig. 4a). The vertical displacement time histories for both cases are plotted in dimensional terms in Fig. 4b and non-dimensional terms in Fig. 4c. The curves coincide as soon as time becomes non-dimensional (multiplied with frequency) and results are presented in terms of the dimensionless ratio w/D. It's interesting to notice that for the applied sinusoidal loading having amplitude half of the caissons' axial capacity, the displayed settlement accumulation after 8 loading cycles is minimal.

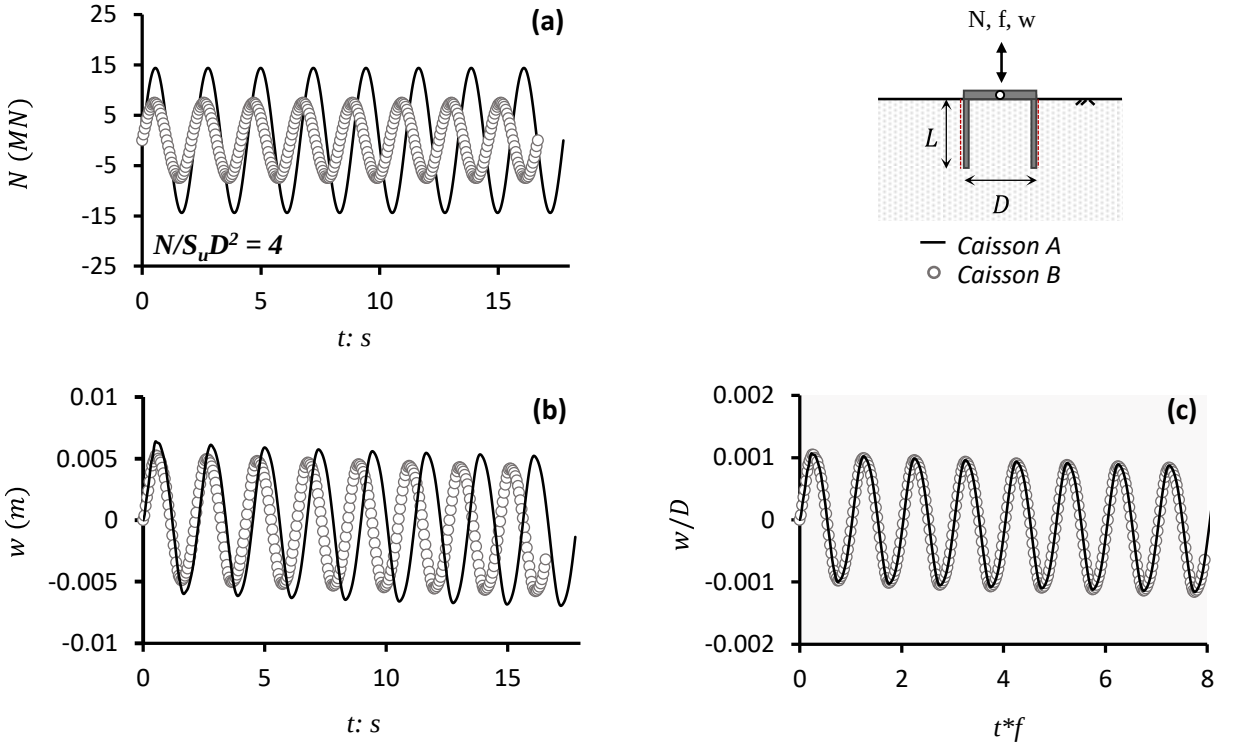

Figure 4. Validation of dimensional formulation for caissons subjected ti dynamic axial cyclic loading: **(a)** Loading time histories and time histories of vertical displacement *w* in **(b)** physical and **(c)** dimensionless terms.

Concurrent Static & Seismic Loading

For this section, the employed FE model is slightly modified to correctly simulate seismic loading. Radiation damping is taken into account by introducing dashpots at the base of the model, with a dashpot constant

$C=\rho V_s A$, where ρ the material density, V_s the shear wave velocity (assuming half-space), and A the effective area of each dashpot. Moreover, appropriate kinematic (MPC) constraints are imposed at the lateral boundaries of the FE model to simulate free-field response of a soil-column subjected to in–plane vertically incident SV waves.

A seismic record from the earthquake of 2013 in Cephalonia Island, Greece is selected for this series of analyses, namely the Lixouri record. The original acceleration time history, which is used as an input for Caisson A analysis, is displayed in Figure 5a (black line). A small duration record, with limited number of cycles, but rather intense, with a maximum acceleration amplitude at α_E = 0.66g and dominant frequency at f_E = 0.71 Hz. For the sake of validation of the postulated dimensional formulations, the analyses of Caisson A and B should yield the same frequency ratio, therefore the record's time scale is manipulated before being applied to Caisson B, to result in a dominant frequency of f_E = 0.76 Hz (Fig. 5a, grey line).

The respective elastic response spectra of the input time histories are presented in Figure 5b for damping ratio equal to ξ = 5%. The additional dimensionless products for seismic analyses now yield f_E/R = 0.017 and $S_u/\rho L\alpha_E$ = 13.8. An initial static loading N corresponding to N/S_uD^2 = 4 is applied to both foundations prior to seismic loading. Time histories of vertical displacement *w* in dimensional (Fig. 5c) and dimensionless terms (Fig. 5d) further validate the postulated dimensional formulation, but also give a first hint of an important observation in this study: as opposed to the previously displayed minimal deformations under symmetric cyclic loading, the caissons now experience an initial settlement of $w_o \approx 8 – 9$ mm (depending on the case) prior to the earthquake loading due to the applied load N, and keep settling thereafter in every single strong seismic pulse.

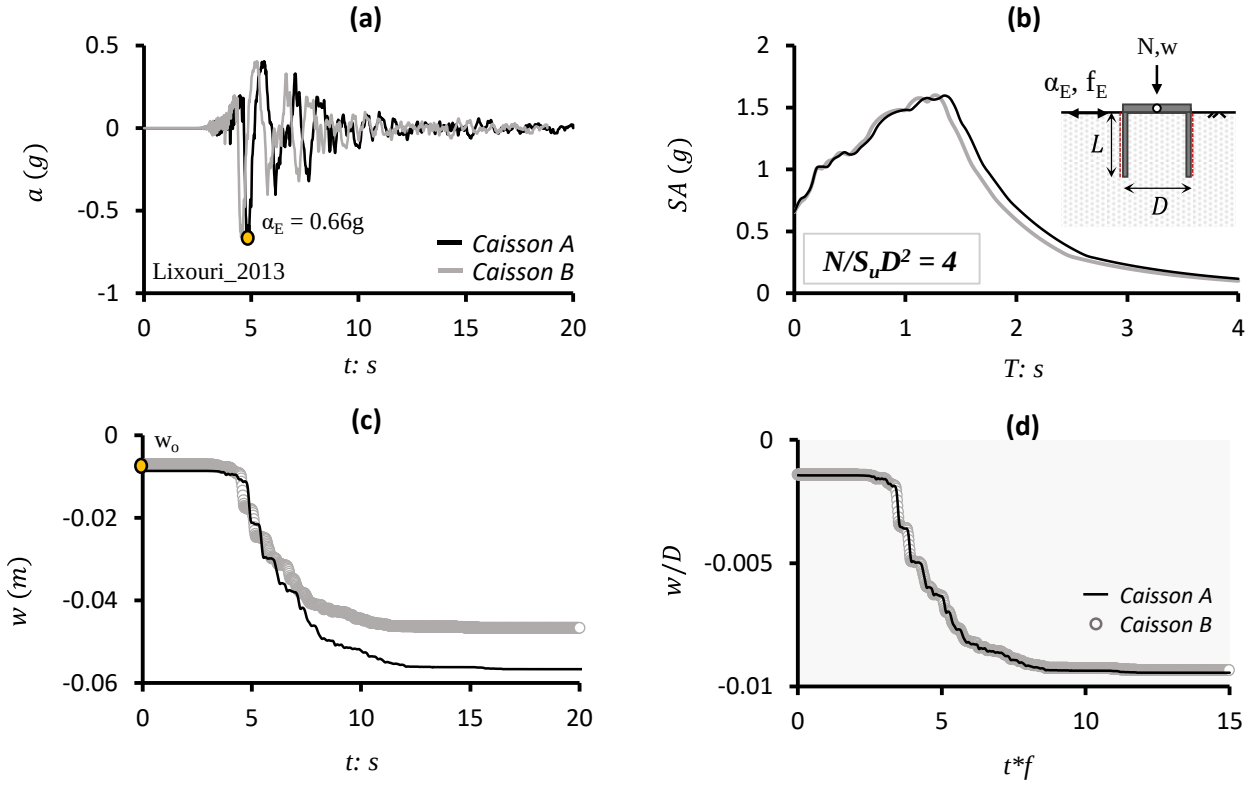

Figure 5. Validation of dimensional formulation for the case of concurrent axial static & seismic loading (N/S_uD^2 = 4): **(a)** Input acceleration time histories at bedrock, **(b)** Respective response spectra at the ground surface for ξ=5%, and time histories of foundation settlement *w* in **(c)** physical and **(d)** dimensionless terms for the Lixouri record.

PARAMETRIC STUDY ON KEY PPARAMETERS AFFECTING CAISSON RESPONSE

The loading protocol type

As indicated already, the examined suction caissons display minor permanent deformations when subjected to pure sinusoidal loading. This section aims to identify how response is affected by the amplitude of the steady force (N_o) applied prior to dynamic cyclic loading, as well as by the amplitude of the subsequent cyclic loading N_c. Caisson A is selected for this set of FE parametric analyses, subjected to the following load cases:

- *Case 1* corresponds to N_o = 0, N_c =14.4 MN (with $N_{max}/S_uD^2 = 4$, where $N_{max} = N_o + N_c$)
- *Case 2* corresponds to N_o =14.4 MN and N_c =7.2 MN (with $N_{max}/S_uD^2 = 6$)
- *Case 3* corresponds to N_o =7.2 MN and N_c =14.4 MN (with $N_{max}/S_uD^2 = 6$)

Loading cases 2 and 3 correspond to a non-symmetrical loading protocol –typically resulted by the combining action of a constant wind force (N_o) and a fluctuating wave thrust (N_c) – of the same maximum load amplitude N_{max} = 21.6. Static loading is applied as a push-down (compressive) force, followed by 8 cycles of sinusoidal loading at a frequency f = 0.451 Hz. MN. Figure 6 depicts the FE analyses results in terms of dimensionless settlement time histories. The trends are clear: once a co-dynamic steady action is imposed, vertical caisson movement cannot anymore change sign under the imposed cyclic load: the caisson acquires an initial settlement due to N_o and keeps settling towards the same direction during subsequent loading. Comparing Cases 2 and 3 (i.e. both having the same N_{max} but different N_o and N_c), it is interesting to observe that although during the first two cycles the caisson accumulated the very same amount of settlement, the rate of settlement produced by Case 3 is marginally higher than that of Case 2 resulting in a slightly higher permanent deformation (which is in the order of w/D = 0.005). Yet, in absolute terms, the amplitude of residual settlement is low – a mere 3 cm – for either loading protocol. Therefore, it is safe to conclude that suction caissons perform well under cyclic loading of any type.

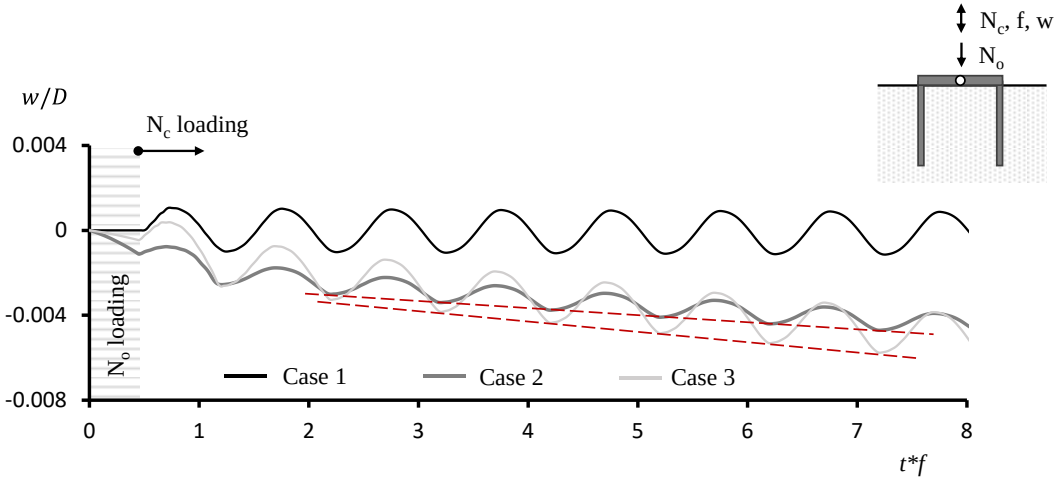

Figure 6. Effect of the initial static loading (N_o) and cyclic loading (N_c) amplitudes on the caisson dynamic response.

The effect of earthquake intensity and bearing load No

The response of Caisson A to the original Lixouri record is compared to the response under two scaled-down versions of the same record, in order to isolate the effect of seismic intensity and exclude effects stemming from other motion characteristics, like the number of cycles or the frequency content. Two levels of co-seismic steady action are considered: the first corresponds to the amount of wind loading that is expected to act on the caisson foundation (of a jacket OWT) during an earthquake (i.e. assuming Normal Sea State) and equals N_o = 7.2 MN (N_o/S_uD^2 = 1.67); the second corresponds to a rather rare event, where the earthquake is combined with a strong steady force equal to N_o = 14.4 MN (almost half the caisson capacity). The second

case, although highly conservative, has been selected as a comprehensive upper-bound scenario to showcase the effect of N_o on the overall caisson response.

Figure 7a plots the acceleration time histories at the ground surface. The original Lixouri record yields a maximum acceleration at the free field equal to α_{max} = 0.59g – a rather strong ground motion– while the scaled-down records result in α_{max} = 0.30g and 0.15g respectively, which are typical of medium intensity and far more frequent seismic events. The effect of earthquake intensity and co-seismic bearing load on the ultimately accumulated settlement are discussed separately in Figures 7b and 7d: in Fig. 7b the N_o/S_uD^2 ratio is constant an equal to 1.67 (corresponding to the case of a lightly loaded caisson) while the amplitude of the earthquake acceleration varies, while in Fig. 7d results for all the above combinations are provided.

As would have been expected, as earthquake intensity increases, so does the cumulative caisson settlement. Moreover, it is a fact that when the caisson is subjected to the strong seismic shaking, accumulation of settlement starts to cease only after *t* = 8s, while for the smaller amplitude records, this very mechanism is suppressed much earlier, already at *t* = 5.5s. Therefore, it appears to be a threshold acceleration value below which the caisson is essentially insensitive to ground shaking and no settlement accumulation takes place (*$\Delta w=0$)*. For the specific example, this threshold may be observed at 0.10g-0.15g. Above this threshold, the incremental settlements *Δw* are non-negligible, while their amplitude is a function of the intensity of the associated seismic pulse. This observation aspired the construction of the chart presented in Fig. 7c (synthesized by pairs of α_i – Δw_i), attempting to provide a primary correlation of acceleration magnitude and incremental settlement for a given N_o/S_uD^2 equal to 1.67. Despite the small scatter (attributed to the fact that parameters other than the acceleration amplitude have not been accounted for, e.g. the frequency of the seismic pulse), a clear trend is observed: incremental *Δw* values increase nonlinearly with increasing acceleration amplitudes, with no evidence of saturation; the stronger the pulse the sharper the caisson sinking.

The second parameter controlling the rate of settlement accumulation of a seismically loaded caisson, is of course the N_o/S_uD^2 index. The greater the initial loading on the caisson (i.e. the higher the N_o/S_uD^2 index), the higher the rate of settlement accumulation (Fig.7d). For the same level of acting acceleration in Fig.7d, the per cycle *Δw* has increased more than double for the assumed variation of N_o/S_uD^2. Earthquake loading leads to a strong difference in response in terms of final accumulated deformations. As a result, the heavily loaded caisson reaches a final settlement of $w_f \approx 60$ mm, whereas for the same record the settlement of the lightly loaded caisson is only $w_f \approx 17$ mm – the settlement that a heavily loaded system would have attained with just half the acceleration amplitude (i.e. α_{max} = 0.30g).

Comment on the Foundation Design with respect to the state of practice

The DNV-OS-J101 standard (2014) suggests that the permanent rotation at the foundation level should not exceed 0.25^o (i.e., 0.0044 rad) to allow continuation of operations. For a jacket structure founded on suction caissons, this figure is represented by the global rotation of the Jacket (θ_{sys}) generated by the differential settlement of the leeward and windward legs. Allowing a number of engineering assumptions, it is possible to correlate θ_{sys} to a threshold (per leg) settlement which, for a realistic OWT jacket structure (for the size of the caissons of the previous paragraph), results a caisson settlement threshold of w_{lim} = 0.04 m.

Combining this code-threshold to the findings of Fig. 7c, it is concluded that an one time seismic event (even a strong one) is not enough to endanger the operability of a Jacket OWT. Risky conditions (that should be accounted in the foundation design) may appear after successive earthquake events, or in the extremely rare event of a strong earthquake taking place at an Extreme Sea State Condition, or in cases of very soft marine clays. It is reminded that the trendline of Fig. 7c corresponds to a stiff clay profile with rigidity ratio E/S_u = 1800 and cannot be used for softer profiles (where rigidity ratios as low as E/S_u = 600 have been measured).

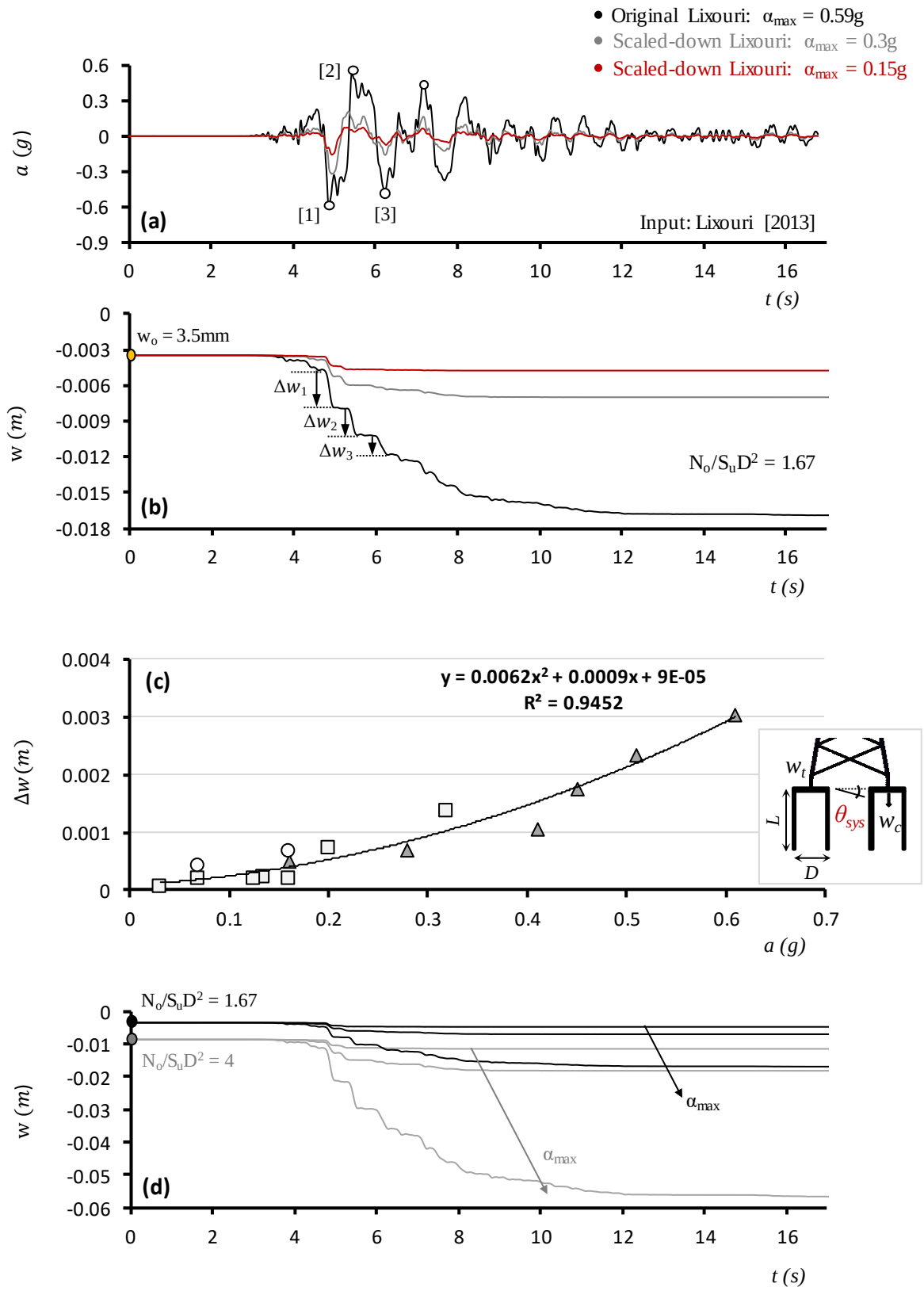

Figure 7. Effect of acceleration amplitude αmax and amplitude of No in concurrent static and seismic loading applied to caisson A. The original and scaled-versions of Lixouri record are employed: (a) acceleration time histories at free field (b) caisson settlements w for $N_o/S_uD^2 = 1.67$, (c) acceleration amplitude α vs. incremental permanent caisson settlements Δw for $N_o/S_uD^2 = 1.67$, (d) comparison of caisson settlements w for $N_o/S_uD^2 = 1.67$ and $N_o/S_uD^2 = 4$.

SEISMIC RESPONSE OF THE ENTIRE SOIL-FOUNDATION-SUPERSTRUCTURE SYSTEM

Having concluded on some key aspects that affect the dynamic response of individual suction caissons, this section aims to present a brief example of the caisson response as part of the entire soil-foundation-superstructure system under seismic loading and identify previously observed trends at the system level. The benchmark example involves an 8MW jacket-supported OWT installed at a water depth of 60m in the Adriatic Sea. The wind turbine and jacket structure characteristics, as well as the environmental load calculations for Normal and Extreme Sea States, are based on the EU Funded Research Program JABACO (Mavrakos, 2016; Von Borstel, T. and Vobeck M., 2016). The foundation soil corresponds to a clay layer of undrained shear strength equal to S_u = 100 kPa, while suction caissons have diameter D = 5.5m and length L = 11m (L/D = 2). The employed 3D FE model of the entire system is illustrated in Figure 8. The general mesh strategy is analogous to the one adopted for the single suction caisson and presented in the previous section. The turbine tower is modelled as a 1-dof system consisting of elastic 3D beam elements (B31) and a concentrated mass at the rotor-nacelle level. The tower is assumed to be rigidly connected to the jacket top and welded connections were allowed between the different jacket components.

In the ensuing, the acceleration time history recorded in L'aquila earthquake in 2009 (bedrock motion) is used as the model excitation (Fig. 9, black curve). The grey time-history in Fig. 9 corresponds to the measured acceleration at the ground surface. The acceleration response spectrum at the ground surface for ξ = 5% is also plotted in the figure, along with the EC-8 design spectrum for the region of interest (A_g = 0.24g). The dominant eigenperiod of the OWT structure equals T_o = 3.65s, indicating a very long-period system with a dominant period far away from the usual earthquake frequencies.

The system is examined under two distinct loading scenarios: the first assumes pure seismic loading, while in the second, the system is subjected to concurrent wind and seismic action, considering 70% of the wind load acting at SLS conditions, i.e. steady wind force of H_{wind} = 872.2kN.

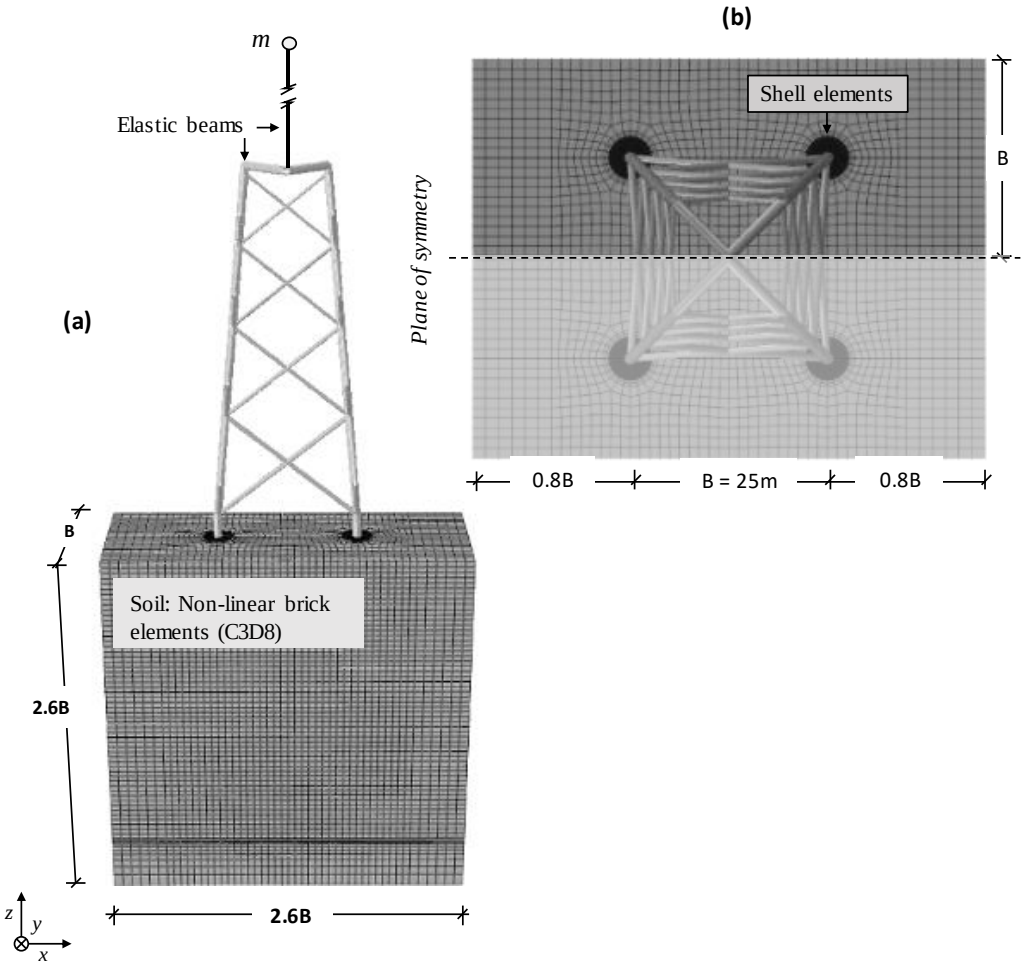

Figure 8. Finite element mesh of the global soil–foundation–jacket structure system.

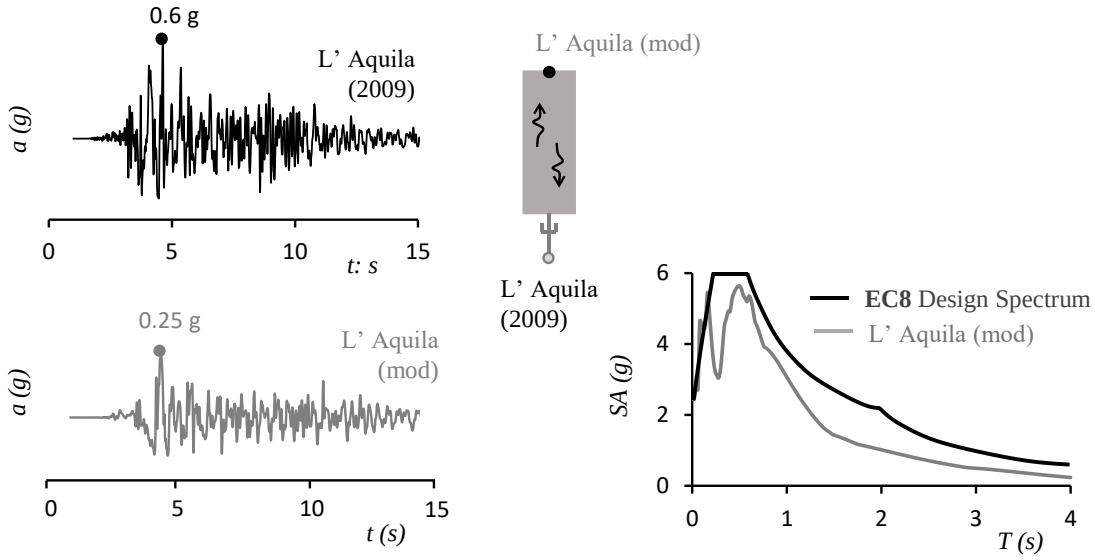

Figure 9. Input acceleration time history (L' Aquila, 2009) and acc. time history at the ground surface, along with its elastic response spectrum. The EC8 design spectrum at the reference location is also provided.

Results are summarized in Figure 10. Figures 10a and 10b depict the acceleration time histories at the nacelle level of the OWT – indistinguishable for both loading scenarios, since the existence (or not) of a constant wind loading doesn't affect the tower acceleration. Apart from that, the low frequency superstructure, filters out the ground shaking acceleration spikes resulting into reduced inertia values that do not exceed 0.15g and are not expected to pose any threat to the mechanical equipment of the rotor, let alone the structural response of the turbine).

Following the discussion of the previous paragraphs, the foundation performance is described as settlement time history in either tensile or compressive leg of the turbine (Fig 10c,d) and system rotation θ_{sys}, defined as $(w_c-w_t)/B$ (Figs.10e,f) : left column for no-wind conditions and right column for the combined wind-earthquake loading case. It is important to observe that accumulation of permanent seismic caisson settlement is generated in both loading cases and the trigger is the same: the coupling of soil shearing along the foundation shaft (generated by the propagating seismic waves) with the shearing caused under the bearing load of the foundation. However, when looking at the foundation rotation time history for the case of pure seismic loading (Fig. 10e), a maximum rotation of 0.3 mrad is observed, which is fully recoverable after the end of shaking. The rate of settlement accumulation is equal in both jacket legs in this case, which causes the two legs to settle at the same rate and hence results in zero system rotation.

On the other hand, under the concurrent action of wind loading, the windward caisson carries increased bearing loading compared to the leeward caisson. This imbalance of bearing loads, creates an imbalance in the rate of settlement accumulation of the two legs, which eventually generates a non-trivial residual rotation θ_E of the order of 0.5 mrad to the system (Fig. 10f).

No doubt it is intriguing to observe that the foundation response of Fig. 10f may be distinguished in two distinct phases. The previous discussion refers entirely to Phase A (the co-seismic phase). During the subsequent Phase B, the turbine continues to oscillate but the caissons don't settle $\Delta w=0$, while the system rotation remains practically constant, fluctuating around a mean value – very similar to Case 2-3 dynamic loading protocols described previously.

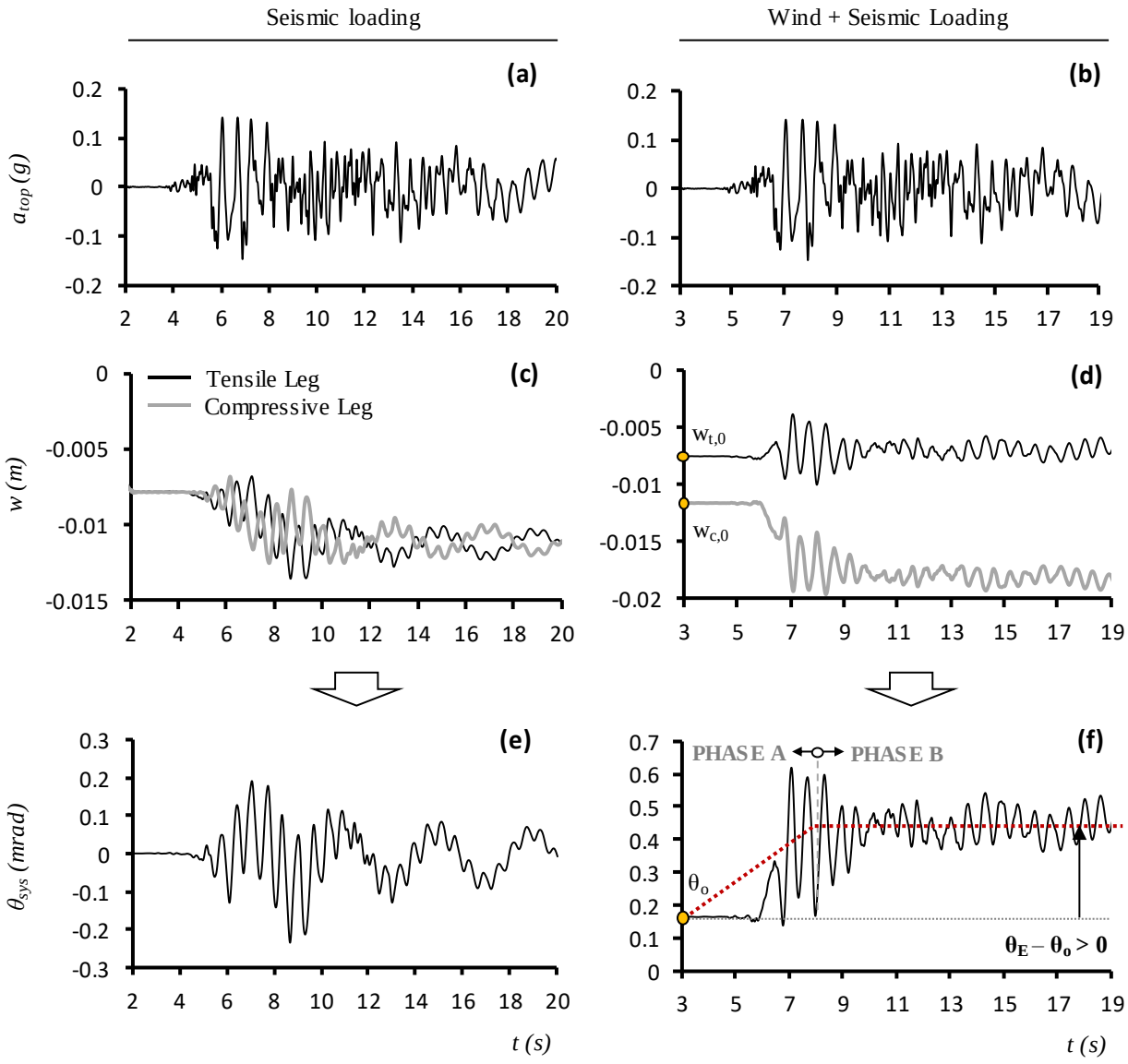

Figure 10. System performance under the L' Aquila record: **(a)**, **(b)** acceleration time histories at nacelle level **(c)**, **(d)** caisson vertical displacements and **(e)**, **(f)** system rotation. Results are comparatively assessed for the case of pure seismic loading and that of concurrent wind and seismic loading.

CONCLUSIONS

The paper analyses the response of suction caissons in clay under dynamic axial loading. Starting with the validation of a proposed dimensional formulation for cyclic dynamic and seismic loading, it continues with a parametric study in a single caisson configuration, which reveals that the accumulation of permanent caisson settlements during dynamic loading is primarily affected by an initially applied steady force and the peak acceleration amplitudes of the seismic motion. Finally, the caissons seismic response is investigated at the system level, using a benchmark example of an 8MW OWT supported on a jacket structure founded on suction caissons. Findings are correlated with observations in previous sections, indicating that the system rotation will display accumulating trends when the seismic loading is combined with a certain amount of wind action.

ACKNOWLEDGMENTS

This research study has been financially supported by the Greek State Scholarship Foundation (IKY Fellowships of Excellence for Postdoctoral Studies in Greece -MIS 5001552.

REFERENCES

ABAQUS 6.14. (2014). Standard user's manual. Dassault Systèmes Simulia Corp., Providence, RI, USA.

Anastasopoulos, I., Gelagoti, F., Kourkoulis, R. and Gazetas, G. (2011). Simplified Constitutive Model for Simulation of Cyclic Response of Shallow Foundations: Validation against Laboratory Tests, Journal of Geotechnical and Geoenv. Eng., ASCE, 137 (12): 1154-1168.

Andersen, K., Dyvik, H.R., Schroder, K., Hansteen, O.E, Bysveen, S. (1993). Field test of anchors in clay II predictions and interpretation. J. Geotech. Geoenviron. 119, 1532–1549.

Bransby M.F., Yun G. (2009). The undrained capacity of skirted strip foundations under combined loading. Géotechnique 59 (2), 115–125.

Byrne, B.W. & Houlsby, G.T. (2003). Foundations for offshore wind turbines. Phil. Trans. R. Soc. London 361, No. 1813, 2909-2930.

Clukey E.C., Morrison M.J. (1993). A centrifuge and analytical study to evaluate suction caissons for TLP applications in Gulf of Mexico. Design and Performance of Deep Foundation, ASCE, pp. 141–156.

Clukey E.C., Morrison, M.J., Gariner, J., Corte, J.F. (1995). The response of suction caisson in normally consolidated clays to cyclic TLP loading conditions. Proceedings of the 27 Th Annual Offshore Technology Conference, Houston,Texas OTC7796, pp. 909–918.

Deng, W., Carter, J.P. (2002). A theoretical study of the vertical uplift capacity of suction caissons. Int. J. Offshore Polar 12 (2), 89–97.

Det Norske Veritas. (2014). Offshore Standard DNV-OS-J101, Design of Offshore Wind Turbine Structures. Det Norske Veritas, Høvik.

Dyvik, R., Andersen, K.H., Hansen, S.B., Christophersen, H.P. (1993). Field test of anchors in clay I description. J. Geotech. Geoenviron. 119, 1515–1531.

Gourvenec S., Barnett S.(2011). Undrained failure envelope for skirted foundations under general loading. Géotechnique 261(3), 263–270.

Iskander, M., El-Gharbawy, S., Olson, R. (2002). Performance of suction caissons in sand and clay. Can. Geotech. J. 39 (3), 576–584

Keawsawasvong S., Ukritchon B. (2016). Finite element limit analysis of pullout capacity of planar caissons in clay. Comput. Geotech. 75, 12–17.

Mana, D.S.K., Gourvenec, S., Randolph, M., Hossain, M.S. (2012). Failure mechanisms of skirted foundations in uplift and compression. Int. J. Phys. Modell. Geotech.12 (2), 47–62.

Mana, D.S.K., Gourvenec, S., Randolph, M.F. (2013). Experimental investigation of reverse end bearing of offshore shallow foundations. Can. Geotech. J. 50, 1022–1033.

Mana D.S.K., Gourvenec S., Martin C.M. (2013). Critical skirt spacing for shallow foundations under general loading. J. Geotech. Geoenviron. 139, 1554–1566.

Mavrakos, S., (2016). Med-Ocean data and hydrodynamic loading for the North Sea and the Mediterranean Sea location. JABACO Development of Modular Steel Jacket for Offshore Windfarms, Deliverable 1.1.

Randolph, M., Gourvenec, S. (2009). Offshore Geotechnical Engineering, Taylor &Francis Spon Press, New York, USA.

Samui, P., Das, S., Kim, D. (2011). Uplift capacity of suction caisson in clay using multivariate adaptive regression spline. Ocean Eng. 38 (17–18), 2123–2127.

Ukritchon B., Keawsawasvong, S. (2016). Undrained pullout capacity of cylindrical suction caissons by finite element limit analysis. Comput. Geotech. 80, 301–311.

Ukritchon B., Wongtoythong P., Keawsawasvong S. (2018). New design equation for undrained pullout capacity of suction caissons considering combined effects of caisson aspect ratio, adhesion factor at interface, and linearly increasing strength. Applied Ocean Research, Volume 75, 1-14.

Von Borstel, T. & Vobeck M. (2016). Preliminary design of reference offshore steel jackets for 8MW and 10MW wind turbines. JABACO Development of Modular Steel Jacket for Offshore Windfarms, Deliverable 1.3.

Vulpe, C. (2015). Design method for the undrained capacity of skirted circular foundations under combined loading: effect of deformable soil plug. Géotechnique 65, No. 8, 669–683.

Wang, X, Yang, X, Zeng, X (2017). Seismic centrifuge modelling of suction bucket foundation for offshore wind turbine. Renew Energy:114.

Wu, X., Hub, Y., Yang, Y., Duan, L., Wang, T., Adcock, T., Jiangh, Z., Gaoi, Z., Lin, Z., Borthwick, A., Liao, S. (2019). Foundations of offshore wind turbines: A review. Renewable and Sustainable Energy Reviews 104, 379–393.